Transient Effects of Band Non-Parabolicity in DGFETs for RF Applications

1st Mathias Pech
Chair for High Frequency Techniques
TU Dortmund
Dortmund, Germany
mathias.pech@tu-dortmund.de

2nd Dirk Schulz
Chair for High Frequency Techniques
TU Dortmund
Dortmund, Germany
dirk2.schulz@tu-dortmund.de

Abstract—The atomistic investigation of modern nanoscale devices for RF applications requires time-resolved simulations, which often come with a high computational burden. Thus, the effective mass approximation is usually employed to reduce the complexity and computation times. Here, a novel approach combining a tight-binding like ansatz with a Quantum Liouville-type Equation is presented, that can effectively take into account any arbitrary energy dispersion relation. It is applied to analyze the charge carrier transport in a DGFET in a single non-parabolic valley and compared to the parabolic case for the stationary and transient cases. As it is shown, the application of the parabolic approximation leads to a severe underestimation of the current densities and does not capture distortion effects when RF amplifier operation is considered.

Index Terms—Computational Nanotechnology, Quantum Transport, Quantum Liouville, Mode Space, DGFET, Non-Parabolicity, Tight-Binding

I. Introduction

By now, a variety of tools for stationary simulations of quantum charge carrier transport exist, such as methods based on non equilibrium Greens function (NEGF) [1] and density matrix approaches [2]. Previous applications of stationary fullband methods on quantum confined field effect transistors have shown that the parabolic approximation of the energy bands severely underestimates the current density [3]. If the time-resolved behavior is to be analyzed for e.g. devices operating in the THz regime, however, the former method becomes less applicable on account of the severe computational burden of the time-dependent Greens function [4]. In contrast, approaches based on Quantum Liouville type Equations (QLTE) have been shown to be an efficient option for the time-resolved case but are usually limited to the assumption of parabolic energy bands. Here, a novel approach based on a QLTE is presented, where an energy dispersion relation similar to that of a tight-binding approach is used instead of the parabolic approximation. By including higher order cosine terms, i.e. more neighbor atoms, effectively any arbitrary energy dispersion can be taken into account. Most importantly, the discretization directly follows from the energy dispersion and no derivatives need be approximated. The resulting staggered grid formulation of the QTLE ([5]) can then be used to obtain a discretization pattern on a conventional uniform grid.

Herein, this formalism is derived starting from the energy dispersion and ultimately leading to a QLTE for arbitrary energy bands on a uniform grid. Subsequently it is applied onto an InAs double gate FET (DGFET) in combination with a mode-space approach (MSA) [6] to obtain the characteristic stationary curves when non-parabolicity in the Γ valley is taken into account. Lastly, its effects in RF amplifier applications are compared to the parabolic approximation case.

II. Incorporating non-parabolic energy dispersion into the QLTE

Introducing non-parabolicity to the density matrix formalism by simply extending the kinetic part of the Hamiltonian to higher order derivatives

$$\hat{\mathcal{H}}_{kin} = \sum_{n=1}^{N} \frac{\hbar^2}{2m_n} \boldsymbol{\nabla}^{2n} \tag{1}$$

has the disadvantage of quickly becoming convoluted after the Weyl transform with many derivative terms that need to be approximated as shown in [7]. With the presented approach, an ansatz based on the tight-binding method is chosen instead, leading to the energy dispersion

$$\hat{\mathcal{H}}_{kin} = E(\mathbf{k}) = E_0 + \sum_{n=0}^{N} c_n \exp(i\mathbf{k}(\mathbf{r_m} - \mathbf{r_n})) \tag{2}$$

assuming s-like orbitals for example with the hopping terms c_n related to the overlap integrals. Assuming dominant charge carrier transport in the x-direction, the kinetic part of the Hamiltonian can be expressed in terms of N cosine functions, where N=1 corresponds to the nearest neighbor approximation, N=2 the next-nearest neighbor approximation, etc.. The energy dispersion in the Γ-valley is thus described by

$$\hat{\mathcal{H}}_{kin} = E(k_x) \overset{\Gamma \to X}{=} E_0 + \sum_{n=0}^{N} c_n \cdot \cos(n \cdot a_0 \cdot k_x) \tag{3}$$

with the atomic distance a_0 and the coupling terms c_n. Inserting (3) into the well known von-Neumann equation (VNE) with k and k' leads to a Liouville operator

$$\hat{\mathcal{L}}_{kin} = \sum_{n=1}^{N} \frac{c_n}{2} \left(e^{\imath n \Delta_{k_x}} - e^{\imath n \Delta_{k_x}} \right) \left(e^{\imath \frac{n}{2} \Delta_{k'_x}} - e^{\imath \frac{n}{2} \Delta_{k'_x}} \right), \tag{4}$$

where the exponential terms can be viewed as the application of a shift operation in a discrete Fourier transform. After a transformation of the operator onto the center of mass coordinates $\tilde{k}_x$ and $\tilde{k}'_x$ and back onto the real space coordinates χ and ξ, an equation for the density matrix elements results [5] as given by

$$\begin{aligned} \imath\hbar \frac{\partial}{\partial t} \underbrace{\rho_{i+\frac{1}{2},j+\frac{1}{2}}}_{\text{q grid}} &= \frac{c_1}{2} \underbrace{\left(\rho_{i,j+1} - \rho_{i,j} - \rho_{i+1,j+1} + \rho_{i+1,j} \right)}_{\text{p grid}} \\ &+ \frac{c_2}{2} \underbrace{\left(\rho_{i-\frac{1}{2},j+\frac{3}{2}} - \rho_{i-\frac{1}{2},j-\frac{1}{2}} - \rho_{i+\frac{3}{2},j+\frac{3}{2}} + \rho_{i+\frac{3}{2},j-\frac{1}{2}} \right)}_{\text{q grid}} \\ &+ \ldots + \underbrace{V_{i+\frac{1}{2},j+\frac{1}{2}} \rho_{i+\frac{1}{2},j+\frac{1}{2}}}_{\text{q grid}} . \end{aligned} \tag{5}$$

Here, the two grids p and q as shown in Fig. 1 with $p(\chi_i, \xi_j) = p_{i,j}$ and analogous indices for q have been introduced along with the potential V that contains the self-consistent Hartree potential, band structure and any external bias. A similar equation can be set up for the density matrix elements $\rho_{i,j}$ corresponding to the p grid on the left hand side. Rewriting the equations in terms of the vectors $\boldsymbol{p}_i = (\rho_{i,1}, \ldots, \rho_{i,N_\xi})^T$ and $\boldsymbol{q}_{i+\frac{1}{2}} = (\rho_{i+\frac{1}{2},\frac{1}{2}}, \ldots, \rho_{i+\frac{1}{2},N_\xi-\frac{1}{2}})^T$ results in a staggered grid formulation of the von-Neumann equation

$$\frac{\partial}{\partial t} \boldsymbol{p}_i = c_1 (\boldsymbol{q}_{i-\frac{1}{2}} - \boldsymbol{q}_{i+\frac{1}{2}}) + c_2 (\boldsymbol{p}_{i-1} - \boldsymbol{p}_{i+1}) + \boldsymbol{V}_i \boldsymbol{p}_i \tag{6}$$

$$\frac{\partial}{\partial t} \boldsymbol{q}_{i+\frac{1}{2}} = c_1 (\boldsymbol{p}_i - \boldsymbol{p}_{i+1}) + c_2 (\boldsymbol{q}_{i-\frac{3}{2}} - \boldsymbol{q}_{i+\frac{3}{2}}) + \boldsymbol{V}_{i+\frac{1}{2}} \boldsymbol{q}_{i+\frac{1}{2}}, \tag{7}$$

where only the nearest and next-nearest neighbor have been included for the sake of clarity. Even though a similar staggered grid scheme can be obtained by means of a rigorous derivation of the Wigner Transport Equation, the occurence of negative charge carrier densities is problematic [8]. By formulating the transport equation in a real space first and performing a plane wave expansion later, these problems can be avoided [5]. The coefficients from (3) directly correlate to the coefficients c_n in (6) and (7) that couple the adjacent grids in transport direction. Therefore, a discretization pattern is obtained through the energy dispersion relation alone, opposed to the more common method of approximating the occuring derivatives as is done in e.g. [7], [9], [10]. In order to avoid any difficulties regarding the boundary conditions of the staggered grid formulation [5], the subgrid $\boldsymbol{q}$ in (7) can be approximated

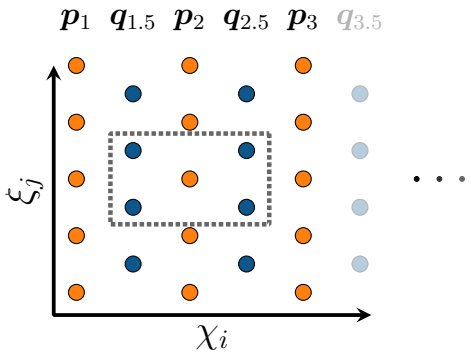

Fig. 1. The staggered grids p and q before the application of a midpoint rule. The dashed box indicates the computational cell for the centermost point if only nearest neighbors are considered for example.

in terms of the subgrid $\boldsymbol{p}$ by the application of a mid-point rule, leading to a uniform grid:

$$\begin{aligned} \frac{\partial}{\partial t} \frac{\boldsymbol{p}_i + \boldsymbol{p}_{i+1}}{2} &\approx c_1 (\boldsymbol{p}_i - \boldsymbol{p}_{i+1}) \\ &+ c_2 \left(\frac{\boldsymbol{p}_{i-1} + \boldsymbol{p}_i}{2} - \frac{\boldsymbol{p}_{i+1} + \boldsymbol{p}_{i+2}}{2} \right) + \boldsymbol{V}_{i+\frac{1}{2}} \frac{\boldsymbol{p}_i + \boldsymbol{p}_{i+1}}{2}. \end{aligned} \tag{8}$$

Finally, a plane wave expansion of the density matrix is performed to facilitate setting up the inflow boundary conditions [11], resulting in a QLTE with band non-parabolicity taken into account. If only the first cosine term, i.e. nearest neighbor is taken into account and the potential $V_{i+\frac{1}{2}}$ is approximated by a midpoint rule as well, the approach is equivalent to the finite volume method described in [10].

III. Application onto DGFETs

A schematic of the DGFET in question is shown in Fig. 2. Regarding the device parameters, the electron affinity of the undoped InAs channel is $\chi = 4.5$ eV. For the oxide and gate material SiO_2 and Ag are chosen, respectively, with a metal work function of $\varphi = 4.74$ eV assumed for the latter. The source and drain regions on either end of the device are n-doped with $N_s = N_d = 2 \cdot 10^{19}$ cm^3.

An uncoupled mode-space approach is applied ([6], [12], [13]), essentially decoupling the confinement and transport directions and leading to a description of the charge carrier transport in subbands. Because the focus is laid first and foremost onto including the non-parabolicity in transport direction, subband eigenvalues and eigenfunctions are assumed for the parabolic case. The resulting eigenvalue problem is solved by using a Lanczos algorithm at each iteration with a spatially varying mass taken into account and Dirichlet boundary conditions on the outside of the oxide. Energy band non-parabolicity is taken into account in the transport direction as well as when determining the density of states and boundary conditions at the contacts. Regarding the boundary conditions, inflow boundary conditions at the drain and source contact are

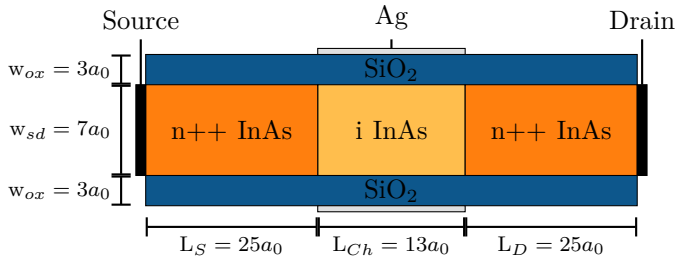

Fig. 2. Schematic of the DGFET with the oxide shown blue, undoped channel in yellow and contacts in orange. To facilitate discretization, all dimensions are given in multiples of $a_0 = 6$ Å.

adopted for the mode-space approach [12], [13]. A complex absorbing potential (CAP) is added onto the conventional potential to avoid reflections resulting from the finite computational domain [14], [15]. Room temperature operation and ballistic charge carrier transport are presumed throughout.

IV. Results

Because of the extensive amount of work that has been done on the conventional Wigner transport equation (WTE), discretization on a uniform grid can be desirable. A comparison for the case of the nearest neighbor approximation of the staggered grid formulation from (6), the uniform grid from (8) and results obtained by a reference quantum transmitting boundary method [16] shows that all resulting output curves coincide well(Fig. 3), justifying the application of the uniform grid description. Therefore, the second order cosine expansion of the bulk energy dispersion of InAs is used and applied for the uniform grid QLTE. As it can be seen from Fig. 4, the dispersion in the Γ valley can be accurately modeled by just 4 cosine terms. For demonstration purposes, the second-order coefficients are utilized.

The self-consistent characteristic output curves are obtained for two gate voltages. The resulting drain-end current densities (Fig. 5) for the parabolic QLTE (P QLTE) coincide with a reference solution obtained by a finite volume Wigner transport equation (FV WTE) [9]. However, when non-parabolicity in the transport direction is taken into account (NP QLTE), much higher current densities are obtained. In order to study the time-resolved behavior, the application as an RF amplifier is studied by keeping the drain-source voltage constant at $V_{ds} = 0.5$ V and applying a harmonic gate voltage $U_g = 0.5V + 0.1 \cdot \sin(2\pi t f)$ at $f = 300$ GHz. As it is shown in Fig. 6, the parabolic approximation underestimates the drain-end current density again but also does not capture the gain compression during the positive half-wave that can be seen in the non-parabolic case. The application of a FFT analysis of the drain-end current densities indicates, that the inclusion of non-parabolicity increases the non-linearity in amplifier operation and excitation of higher order harmonics (Fig. 7).

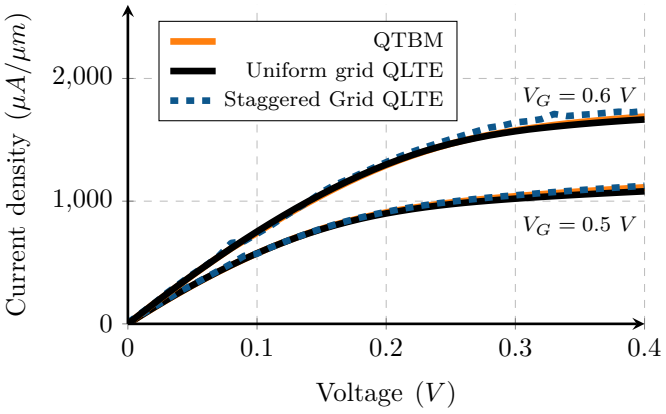

Fig. 3. The drain-end current densities for the nearest-neighbor QLTE on a staggered grid and a uniform grid are in good agreement with reference results obtained by the quantum transmitting boundary method (QTBM). The drain and source regions have been lengthened and permittivity is increased towards the contacts to ensure good convergence for the staggered grid case.

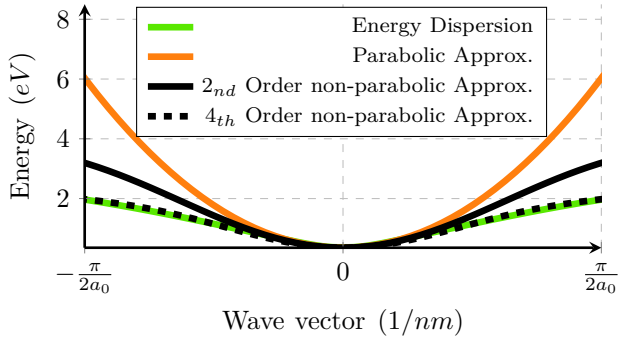

Fig. 4. Bulk energy dispersion in the Γ valley for InAs as obtained by a sp3s* tight-binding calculation with the parabolic and non-parabolic approximation with $N = 2$ and $N = 4$ cosine terms.

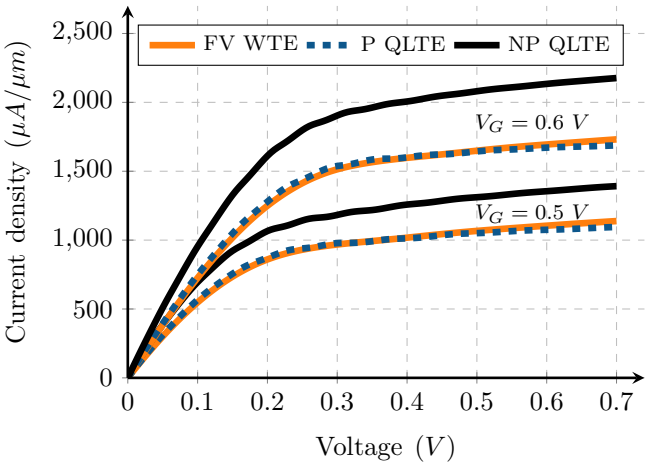

Fig. 5. The drain-end current density for the parabolic QLTE (P QLTE)is in good accordance with a result obtained by a finite volume Wigner approach (FV WTE). However, the current density is underestimated by more than 20 % when compared to the non-parabolic case (NP QLTE).

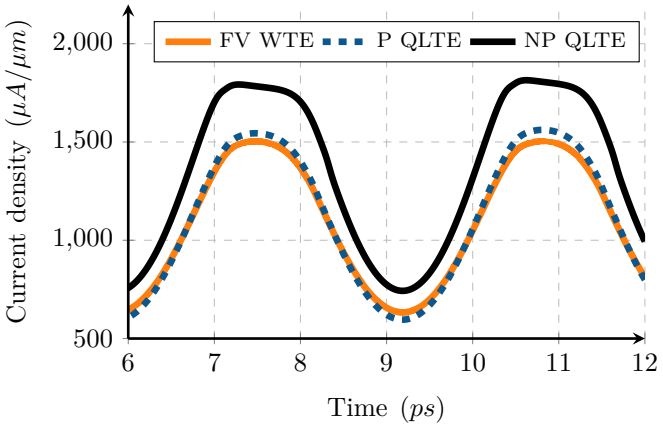

Fig. 6. The inclusion of non-parabolicity leads to compression during the positive half wave. This effect is not seen in the parabolic cases for the QLTE and finite volume Wigner approach, which coincide well.

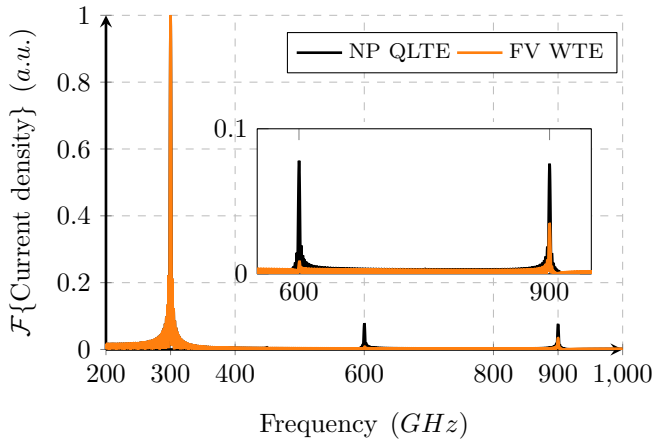

Fig. 7. The normalized spectra of the drain-end current densities show that the non-parabolicity leads to an increased excitation of higher order harmonics in amplifier operation as depicted in the inset.

V. Discussion

The proposed approach was shown to be well suited to model the stationary and transient charge carrier transport in semiconductors with non-parabolic energy dispersion. By utilizing an approach similar to a tight-binding method, it retains an atomistic description of the charge carrier transport when applied onto a QLTE. The band non-parabolicity was shown to significantly affect the stationary and time-dependent carrier transport, with an increased excitation of higher-order harmonics in amplifier operation. As non-parabolicity in the confinement direction was neglected here, it should be taken into account in future works. The approach should be extended onto heterostructures and multiband models, allowing for the time-dependent modeling of multivalley transport for the investigation of e.g. intervalley mixing in resonant tunneling diodes.

Acknowledgment

This work was supported by the German Research Funding Association Deutsche Forschungsgemeinschaft (DFG) under Grant SCHU 1016/8. Computing time was provided on the LiDO3 cluster at TU Dortmund, partially funded in the course of the Large-Scale Equipment Initiative by the DFG as project 271512359.

References

[1] S. Steiger, M. Povolotskyi, H.-H. Park, T. Kubis, and G. Klimeck, "Nemo5: A parallel multiscale nanoelectronics tool," IEEE Transactions on Nanotechnology, 01 2011.

[2] J. Weinbub and D. K. Ferry, "Recent advances in wigner function approaches," Applied Physics Reviews, vol. 5, no. 4, p. 041104, 2018.

[3] M. Luisier, A. Schenk, and W. Fichtner, "Three-dimensional full-band simulations of si nanowire transistors," in 2006 International Electron Devices Meeting, 2006, pp. 1–4.

[4] B. Gaury, J. Weston, M. Santin, M. Houzet, C. Groth, and X. Waintal, "Numerical simulations of time-resolved quantum electronics," Physics Reports, vol. 534, no. 1, pp. 1–37, jan 2014.

[5] M. Pech and D. Schulz, "Investigation of a staggered grid formulation of the wigner transport equation for complex band structures," Book of Abstracts of the International Wigner Workshop (IWW), pp. 26–27, 2023, ISBN: 978-3-9504738-5-8.

[6] R. Venugopal, Z. Ren, S. Datta, M. S. Lundstrom, and D. Jovanovic, "Simulating quantum transport in nanoscale transistors: Real versus mode-space approaches," Journal of Applied Physics, vol. 92, no. 7, pp. 3730–3739, 2002.

[7] K.-Y. Kim and B. Lee, "Wigner function formulation in non-parabolic semiconductors using power series dispersion relation," Journal of Applied Physics, vol. 86, no. 9, pp. 5085–5093, 11 1999.

[8] R. Mains and G. Haddad, "An accurate re-formulation of the wigner function method for quantum transport modeling," Journal of Computational Physics, vol. 112, no. 1, pp. 149–161, 1994.

[9] L. Schulz and D. Schulz, "Formulation of a phase space exponential operator for the wigner transport equation accounting for the spatial variation of the effective mass," Journal of Computational Electronics, vol. 19, 2020.

[10] L. Schulz, B. Inci, M. Pech, and D. Schulz, "Subdomain-based exponential integrators for quantum liouville-type equations," Journal of Computational Electronics, vol. 20, no. 6, pp. 2070–2090, 2021.

[11] W. R. Frensley, "Boundary conditions for open quantum systems driven far from equilibrium," Rev. Mod. Phys., vol. 62, pp. 745–791, Jul 1990.

[12] H. Jiang and W. Cai, "Effect of boundary treatments on quantum transport current in the green's function and wigner distribution methods for a nano-scale dg-mosfet," Journal of Computational Physics, vol. 229, no. 12, pp. 4461–4475, 2010.

[13] L. Schulz and D. Schulz, "Time-resolved mode space based quantum-liouville type equations applied onto dgfets," in 2020 International Conference on Simulation of Semiconductor Processes and Devices (SISPAD), 2020, pp. 331–334.

[14] ——, "Complex absorbing potential formalism accounting for open boundary conditions within the wigner transport equation," IEEE Transactions on Nanotechnology, vol. 18, pp. 830–838, 2019.

[15] ——, "Numerical analysis of the transient behavior of the non-equilibrium quantum liouville equation," IEEE Transactions on Nanotechnology, vol. 17, no. 6, pp. 1197–1205, 2018.

[16] C. S. Lent and D. J. Kirkner, "The quantum transmitting boundary method," Journal of Applied Physics, vol. 67, no. 10, pp. 6353–6359, 05 1990.